The EMBO Journal vol.14 no.5 pp.876–883, 1995

Mechanism of dysfunction of two nucleotide binding domain mutations in cystic fibrosis transmembrane conductance regulator that are associated with pancreatic sufficiency

David N.Sheppard, Lynda S.Ostedgaard, Michael C.Winter and Michael J.Welsh[1]

Howard Hughes Medical Institute, Departments of Physiology and Biophysics and Internal Medicine, University of Iowa College of Medicine, Iowa City, IA 52242, USA

[1]Corresponding author

Communicated by A.Smith

Variability in the severity of cystic fibrosis (CF) is in part due to specific mutations in the CF transmembrane conductance regulator (CFTR) gene. To understand better how mutations in CFTR disrupt Cl^- channel function and to learn about the relationship between genotype and phenotype, we studied two CF mutants, A455E and P574H, that are associated with pancreatic sufficiency. A455E and P574H are located close to conserved ATP binding motifs in CFTR. Both mutants generated cAMP-stimulated apical membrane Cl^- currents in heterologous epithelial cells, but current magnitudes were reduced compared with wild-type. Patch–clamp analysis revealed that both mutants had normal conductive properties and regulation by phosphorylation and nucleotides. These mutants had normal or increased Cl^- channel activity: A455E had an open-state probability (P_o) similar to wild-type, and P574H had an increased P_o because bursts of activity were prolonged. However, both mutants produced less mature glycosylated protein, although levels were greater than observed with the ΔF508 mutant. These changes in channel activity and processing provide a quantitative explanation for the reduced apical Cl^- current. These data also dissociate structural requirements for channel function from features that determine processing. Finally, the results suggest that the residual function associated with these two mutants is sufficient to confer a milder clinical phenotype and infer approaches to developing treatments.

Key words: biosynthesis/CFTR/Cl^- channel/cystic fibrosis/mutations

Introduction

Cystic fibrosis (CF) is caused by mutations in a single gene encoding the CF transmembrane conductance regulator (CFTR; Riordan *et al.*, 1989). However, the disease has a variable clinical phenotype, with the state of pancreatic function being the most clearly identified variable (Kristidis *et al.*, 1992; Welsh *et al.*, 1994). Most patients suffer pancreatic failure and are termed pancreatic insufficient (PI), but some retain significant pancreatic function and are termed pancreatic sufficient (PS). In general, PS patients tend to have less severe disease. Several studies have suggested a relationship between genotype and the clinical phenotype (PS and PI; Kristidis *et al.*, 1992; The Cystic Fibrosis Genotype–Phenotype Consortium, 1993; Gan *et al.*, 1994; Veeze *et al.*, 1994). The PI phenotype occurs in patients who have two 'severe' mutations, whereas the PS phenotype occurs in patients who have either two 'mild' mutations or one 'mild' mutation and one 'severe' mutation (Kristidis *et al.*, 1992).

To understand the relationship between genotype and clinical phenotype, it is necessary to learn how mutations in CFTR disrupt its function. Previous studies have shown that CFTR functions as a Cl^- channel that is regulated by phosphorylation and intracellular nucleotides (for reviews see Collins, 1992; Welsh *et al.*, 1992; Riordan, 1993). The most common CF-associated mutation (ΔF508) is located in the first nucleotide binding domain (NBD1) of CFTR. This mutant is misprocessed and fails to traffic to the apical cell membrane (Cheng *et al.*, 1990; Denning *et al.*, 1992b; Kartner *et al.*, 1992). As a result, there is no cAMP-regulated Cl^- permeability in the cell membrane. Patients homozygous for ΔF508 are PI. In contrast, three mutations (R117H, R334W and R347P) in the first membrane-spanning domain (MSD1) are associated with the PS phenotype (Kristidis *et al.*, 1992; The Cystic Fibrosis Genotype–Phenotype Consortium, 1993). Each of these mutants is correctly processed and delivered to the cell membrane where they form regulated Cl^- channels. However, Cl^- efflux through individual channels is impaired and mutations at residue R347 likely disrupt the multi-ion pore behavior of the channel (Sheppard *et al.*, 1993; Tabcharani *et al.*, 1993). These mutant channels probably retain sufficient residual Cl^- channel function to prevent complete pancreatic failure and to confer a milder clinical phenotype.

Genotyping of a large number of CF patients has identified mutations in other domains of CFTR that are also associated with a PS phenotype. Two such mutations are located within NBD1: A455E and P574H (Kerem *et al.*, 1990; Kristidis *et al.*, 1992). Although these mutations are uncommon, A455E accounts for ~10% of CF chromosomes in some areas of The Netherlands and in the Saguenay-Lac St Jean region of Quebec, Canada (Rozen *et al.*, 1992; Gan *et al.*, 1994). A455E and P574H affect residues in NBD1 that are located close to the Walker A (residues 458–464) and B (residues 568–572) motifs, respectively. These highly conserved motifs are thought to be involved in the interaction between the NBDs and intracellular nucleotides that regulates channel opening and closing (Walker *et al.*, 1982). Therefore, we tested the hypothesis that A455E and P574H might alter the function of CFTR Cl^- channels. We sought to understand the mechanism of dysfunction of these channels and thus the reason why these mutations are associated with a milder clinical phenotype.

© Oxford University Press

Results

Expression of A455E and P574H generates cAMP-activated Cl^- currents

To learn whether A455E and P574H could form regulated Cl^- channels in epithelia, we expressed these mutants in Fischer rat thyroid (FRT) epithelia (Nitsch and Wollman, 1980; Sheppard *et al.*, 1993, 1994a). For comparison, we also expressed wild-type CFTR and ΔF508. We used methods that we had developed previously to assess the function of wild-type and mutant CFTR in the apical membrane of FRT epithelia (Sheppard *et al.*, 1994a). To measure apical membrane Cl^- current, we permeabilized the basolateral membrane to monovalent ions using nystatin and imposed a large transepithelial Cl^- concentration gradient (Sheppard *et al.*, 1993, 1994a). Under these conditions, changes in current generated by cAMP agonists represent Cl^- flowing through CFTR Cl^- channels in the apical membrane. Figure 1 shows that A455E and P574H generated cAMP-stimulated apical Cl^- currents, but ΔF508 did not. However, the magnitude of current generated by A455E and P574H was <20% that of wild-type CFTR in the rank order: wild-type CFTR >> P574H > A455E > ΔF508.

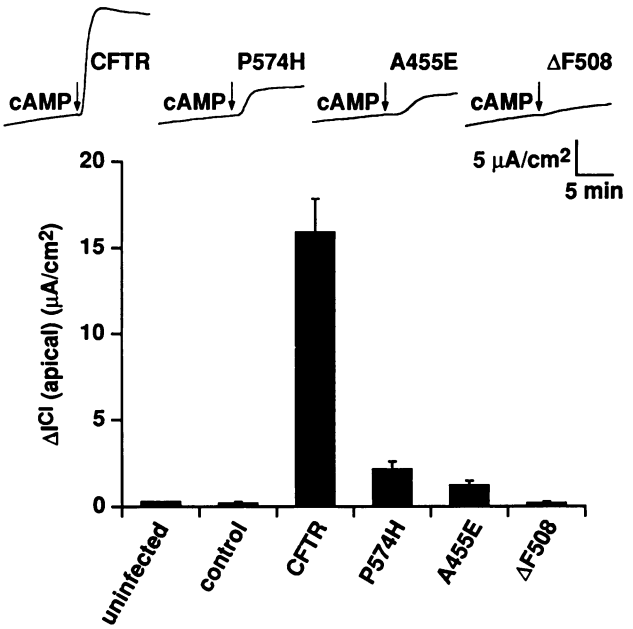

Fig. 1. cAMP agonists activate apical membrane Cl^- currents in FRT epithelia expressing A455E and P574H. Tracings at the top show the representative recordings of apical Cl^- current; arrows indicate the point of addition of cAMP agonists (10 μM forskolin and 100 μM IBMX). Bar graph shows the magnitude of cAMP-stimulated apical Cl^- current generated by wild-type and mutant CFTR. Data are the change in current [ΔI^{Cl}(apical)] measured 3 min after the addition of cAMP agonists. FRT epithelia were infected with identical concentrations of recombinant viruses (MOI = 5). Results are the mean ± SEM of 10 observations for each mutant.

When we expressed A455E and P574H in HeLa cells and studied them with the whole-cell patch–clamp technique, we found properties qualitatively similar to those observed with wild-type CFTR (Welsh *et al.*, 1992; Riordan, 1993). Figure 2 shows data from studies of P574H; similar results were obtained with A455E (data not shown). Whole-cell currents were reversibly activated by cAMP agonists, were time-independent, had relatively linear current–voltage ($I-V$) relationships, and were anion-selective, with anion permeability and conductance sequences of $Br^- \geq Cl^- > I^-$. However, the magnitude of cAMP-activated whole-cell Cl^- current was reduced compared with that of wild-type. For example, when wild-type CFTR was expressed in HeLa cells using conditions similar to those used for FRT studies, cAMP agonists stimulated Cl^- current in five out of five cells and the cAMP-induced change in current was 35.3 ± 3.9 pA/pF (cell capacitance = 27.3 ± 1.7 pF). In contrast, when P574H was expressed using the same conditions, cAMP agonists stimulated current in only five out of 12 cells,

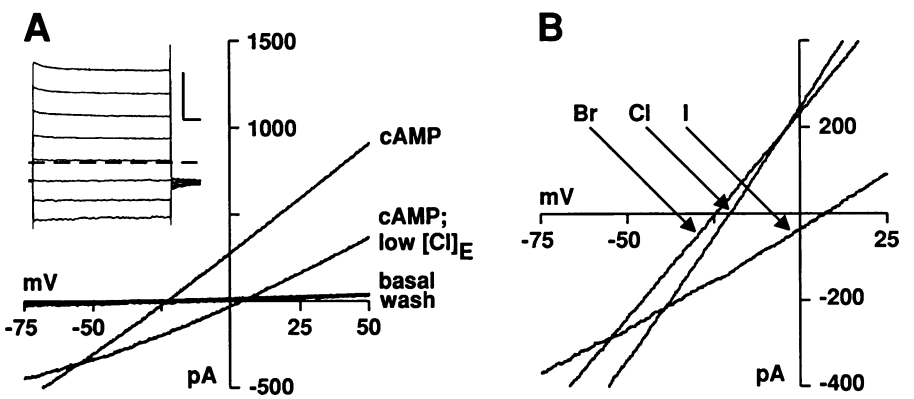

Fig. 2. Whole-cell properties of P574H. (**A**) Current–voltage ($I-V$) relationships of whole-cell currents under basal conditions, 2 min after the addition of cAMP agonists [10 μM forskolin, 100 μM IBMX and 500 μM 8-(4-chlorophenylthio)-adenosine 3′:5′-cyclic monophosphate sodium salt] to the bath solution, and after removing cAMP (wash). The reversal potential (E_{rev}) of baseline-subtracted cAMP-stimulated currents was −27 ± 2 mV (n = 5); predicted E_{Cl} = −32 mV; P_{Na}/P_{Cl} = 0.07 ± 0.03; n = 5. $I-V$ relationships under basal and wash conditions are largely hidden under the abscissa. 'cAMP; low $[Cl]_E$' indicates the $I-V$ relationship when the bath Cl^- concentration was reduced to 20 mM (NaCl replaced with Na aspartate) in the presence of cAMP agonists. $I-V$ relationships were obtained by a 400 ms ramp of voltage; the holding voltage was −40 mV. The inset shows the cAMP-stimulated whole-cell Cl^- currents from the same cell following subtraction of the basal currents. The holding voltage was −40 mV and the voltage was stepped from −80 to +60 mV in 20 mV increments. The dashed line represents the zero current level. The scale bars are 500 pA and 50 ms, respectively. (**B**) $I-V$ relationships of cAMP-stimulated whole-cell currents recorded in the presence of 140 mM Cl^-, Br^- or I^- in the bath solution. Permeability ratios, P_X/P_{Cl}, were: I^-, 0.44 ± 0.05; Br^-, 1.27 ± 0.08. Conductance ratios, G_X/G_{Cl}, were: I^-, 0.45 ± 0.06; Br^-, 0.98 ± 0.07 (n = 5); values were calculated as described previously (Sheppard *et al.*, 1993).

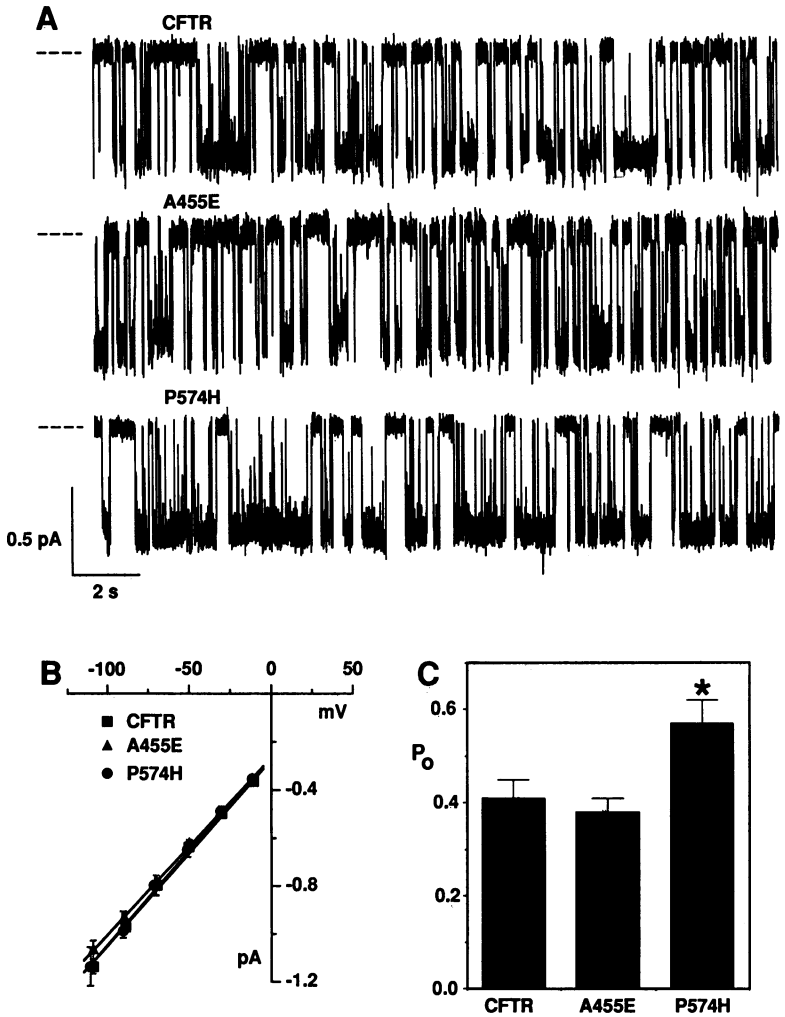

Fig. 3. Single-channel properties of A455E and P574H. (**A**) Representative single-channel recordings are from excised inside-out membrane patches from HeLa cells transiently expressing wild-type CFTR, A455E or P574H. The intracellular solution contained MgATP (0.88 mM) and the catalytic subunit of PKA (75 nM). Each trace is 20 s long. Dashed lines indicate the closed state; downward deflections correspond to channel openings. The voltages were −45 (CFTR), −46 (A455E) or −47 mV (P574H). (**B**) Single-channel $I-V$ relationships of CFTR (■), A455E (Δ) and P574H (●). Data points are the mean ± SEM of three to six values at each voltage, determined in the presence of 0.88 mM MgATP and 75 nM PKA. Lines are the mean slope conductance calculated from the slope conductance of individual experiments. Conductance was CFTR 7.76 ± 0.14, A455E 7.40 ± 0.25 and P574H 7.84 ± 0.26 pS; n = 6. (**C**) Single-channel open-state probability (P_o) determined in the presence of 0.88 mM MgATP and 75 nM PKA (n = 8 for each). The asterisk indicates a value different from wild-type CFTR ($P < 0.016$). The voltage was −50 mV.

and in those cells the cAMP-stimulated change in current was 9.1 ± 4.6 pA/pF (P = 0.02, cell capacitance = 29.3 ± 2.2 pF).

Single-channel properties of A455E and P574H

To determine why A455E and P574H generated less macroscopic Cl^- current, we examined their single-channel properties in excised, inside-out patches of membrane. Figure 3A shows single-channel currents of wild-type and mutant CFTR following phosphorylation with cAMP-dependent protein kinase (PKA). The tracings show that the single-channel current amplitudes of A455E and P574H were similar to that of wild-type CFTR. Figure 3B shows that the single-channel slope conductance of these mutants did not differ from that of wild-type. These data contrast with our previous finding that mutations in MSD1 that are associated with a PS phenotype have altered single-channel conductances (Sheppard *et al.*, 1993).

Figure 3A shows that A455E had a pattern of gating that closely resembled that of wild-type CFTR. This pattern is characterized by bursts of activity containing brief flickery closures, separated by longer closures between bursts. However, P574H showed a different pattern of activity. The most readily apparent change was an increase in the duration of bursts of activity. More subtle was an increase in the duration of closures between bursts.

To quantitate the activity of these mutants, we measured single-channel open-state probability (P_o). Figure 3C shows that the P_o of A455E was similar to that of wild-type CFTR, whereas the P_o of P574H was increased significantly. For both wild-type and mutant CFTR, P_o was relatively voltage-independent (data not shown), consistent with the time independence of whole-cell currents.

To understand better the behavior of these channels, we examined the gating kinetics of phosphorylated wild-type and mutant Cl^- channels in patches of membrane containing only a single channel. We focused primarily on P574H to determine why the P_o of this mutant was greater than that of wild-type CFTR. Maximum likelihood

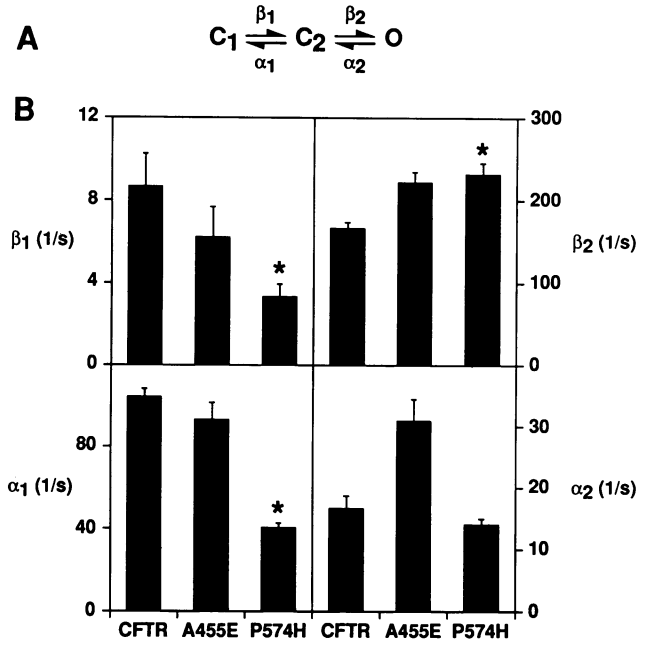

Fig. 4. Effect of A455E and P574H on single-channel kinetics. (**A**) A linear three-state model which describes the behavior of the phosphorylated wild-type CFTR Cl^- channel (Winter *et al.*, 1994). States C_1, C_2 and O represent two closed states and one open state, respectively, while β_1, β_2, α_1 and α_2 represent the four rate constants describing transitions between the open and closed states. (**B**) Effect of A455E and P574H on rate constants determined by the maximum likelihood fit to the model in (A). Data are from four CFTR, two A455E and six P574H single-channel patches. The rate constants were determined in the presence of 0.88 mM MgATP and 75 nM PKA. The voltages were -50 ± 2 (CFTR), -48 ± 1 (P574H) and -47 ± 1 mV (A455E). The asterisks indicate values significantly different from those of wild-type CFTR ($P < 0.05$).

analysis has demonstrated that the activity of single phosphorylated wild-type channels can be described by the linear three-state model shown in Figure 4A (Winter *et al.*, 1994). In this model, C_1 represents the long-closed state separating bursts of channel activity and $C_2 \Leftrightarrow O$ represents the bursting state in which channel openings (O) are interrupted by brief flickery closures (C_2). Transitions between the three states are described by the rate constants β_1, β_2, α_1 and α_2. Our previous results have indicated that intracellular ATP regulates CFTR at the transition between C_1 and C_2: as the ATP concentration increases, β_1 increases. In contrast, the other transitions were not altered significantly by ATP (Winter *et al.*, 1994).

The effect of P574H on the rate constants is summarized in Figure 4B. The major effect of the P574H mutation was to decrease β_1 and α_1 to ~40% of wild-type values. The mutation also increased β_2 but did not change α_2. The decrease of β_1 slows the transition from the long-lived closed state to the bursting state. In contrast, the decrease in α_1 delays exit from the bursting state to the long-lived closed state, thereby increasing burst duration. The increase in β_2, the transition rate between the short-lived closed state and the open state, further increases the duration of bursts. These changes explain the observed increase in the duration of bursts (Figure 3A). This point can also be appreciated from an examination of the equation describing mean burst duration ($\bar{T}_b$):

$$\bar{T}_b = [\beta_2/(\alpha_1\alpha_2)] + (1/\alpha_1) - (1/\beta_2).$$

All of the changes in rate constants produced by P574H tend to increase $\bar{T}_b$. The increase in burst duration is responsible for the increase in P_o (Figure 3C), but it is partially offset by the decreased frequency with which P574H channels move into the bursting state (i.e. the decreased β_1).

In two experiments we examined the gating kinetics of single phosphorylated A455E Cl^- channels. A455E did not alter β_1 or α_1, but tended to increase β_2 and α_2 in both experiments (Figure 4B). This result indicates that the opening and closing transitions within a burst of activity were faster, but is consistent with the lack of a significant change in P_o (Figure 3C) because transitions between the long-lived closed state and the bursting state are unaltered.

These data show that two different mutations in NBD1, both associated with the PS phenotype, have distinct effects on the gating kinetics of single phosphorylated CFTR Cl^- channels.

Regulation of A455E and P574H by intracellular nucleotides

Intracellular MgATP regulates CFTR through interactions with the NBDs. In previous studies it was shown that several other CF-associated mutations in the NBDs had altered regulation by intracellular MgATP. For example, G551S, G1244E, S1255P and G1349D had a markedly reduced P_o at all concentrations of MgATP tested, and S1255P was less potently stimulated by MgATP (Anderson and Welsh, 1992; Smit *et al.*, 1993). Therefore, we tested the hypothesis that ATP-dependent regulation of A455E and P574H was altered. Figure 5A shows that as the concentration of MgATP increased, the P_o of wild-type and mutant CFTR increased. At each concentration of MgATP tested, A455E had P_o values similar to those of wild-type CFTR, whereas P574H had higher values of P_o.

Previous data have suggested that ADP inhibits the activity of CFTR Cl^- channels through an interaction with NBD2 (Anderson and Welsh, 1992). Figure 5B shows that ADP (1 mM) produced an equivalent inhibition of wild-type CFTR, A455E and P574H. This result suggests that these NBD1 mutants do not alter the interaction of ADP with CFTR.

Analysis of the processing of A455E and P574H

The data indicate that the reduced apical membrane Cl^- current produced by A455E and P574H cannot be attributed to the reduced function of single mutant channels. Therefore, we asked whether these mutants might be misprocessed so that they fail to traffic to the Golgi complex and then to the cell membrane. This process can be evaluated by analyzing the glycosylation state of the protein (Cheng *et al.*, 1990). We assessed the production of the mature, fully glycosylated form of CFTR (band C) by expressing the mutants in HeLa and FRT cells, immunoprecipitating the protein and phosphorylating it with PKA and [γ-^{32}P]ATP (Cheng *et al.*, 1990). Figure 6A shows a representative time course of protein production in HeLa cells expressing wild-type and mutant CFTR. The band C form of CFTR was readily detectable in wild-type CFTR by 5 h after infection. However, band C production was reduced in A455E and P574H and was not apparent until 12–24 h after infection, and only then as a faint

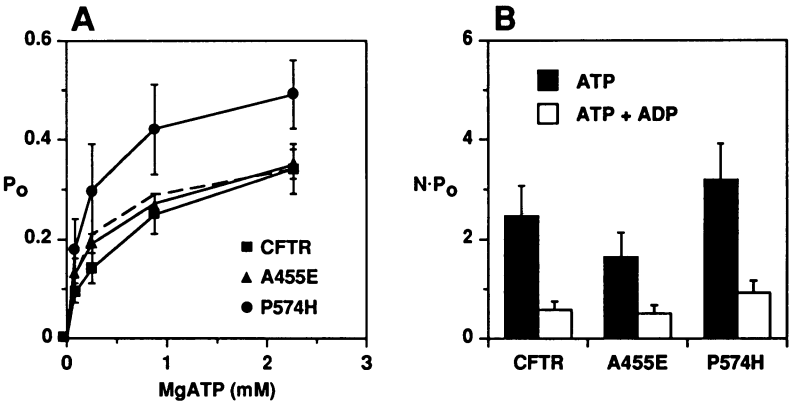

Fig. 5. Effects of MgATP concentration and ADP on the activity of phosphorylated A455E and P574H channels. (**A**) Relationship between P_o and intracellular MgATP concentration for A455E, P574H and wild-type CFTR Cl^- channels. Data points are the mean ± SEM of n = 4–6 for CFTR (■), n = 5 for A455E (▲) and n = 3–5 for P574H (●) at each concentration. The voltages were −86 ± 1 (CFTR), −49 ± 2 (A455E) and −49 ± 1 mV (P574H). Data for wild-type CFTR are from Sheppard *et al.* (1994b). (**B**) Effect of intracellular ADP on the activities of CFTR, A455E and P574H Cl^- channels. $N \times P_o$ values were calculated before and after the addition of ADP (1 mM) to an intracellular solution containing MgATP (0.88 mM). Values are the mean ± SEM of n = 4 for CFTR, A455E and P574H; the voltages were −49 ± 1 (CFTR), −48 ± 2 (A455E) and −52 ± 1 mV (P574H). Percent inhibition of $N \times P_o$ by 1 mM ADP was CFTR 77 ± 3, A455E 70 ± 3 and P574H 75 ± 6%. We measured a similar inhibition (74 ± 6%) of CFTR current when we measured P_o in patches containing fewer channels (Sheppard *et al.*, 1994b).

band. As a control, we also expressed ΔF508, which failed to produce detectable band C protein even at 24 h after infection. Similar results were observed in FRT cells (data not shown). Figure 6B shows the ratio of counts in band C to those in bands A plus B at 24 h. Although the production of mature band C protein was greatly reduced in A455E and P574H, it was greater than that observed with ΔF508.

Discussion

Relationship between apical membrane Cl^- currents and the properties of mutant CFTR

Because the A455E and P574H mutations cause CF, we hypothesized that Cl^- transport would be reduced in cells expressing these mutants. When we expressed the mutant proteins in the apical membrane of FRT epithelia, we found that cAMP-stimulated Cl^- current was decreased compared with that of wild-type CFTR. Our studies of the single-channel properties and the processing of these mutants provide a molecular explanation for the reduced apical Cl^- current. Apical membrane Cl^- current [I^{Cl}(apical)] is determined by the product of the number of Cl^- channels in the apical membrane (N), the single-channel current amplitude (i) and the probability (P_o) that a single channel is open: $I^{Cl}(\text{apical}) = N \times i \times P_o$. If we set each of these variables to 100% for wild-type CFTR, we can then compare the apical Cl^- current generated by wild-type and ΔF508 CFTR with that produced by A455E and P574H. Table I presents values of each variable, the predicted value of I^{Cl}(apical) determined by calculating $N \times i \times P_o$ and the observed value of I^{Cl}(apical). Differences between observed and predicted values may reflect errors resulting from the calculation of N based on the amount of CFTR present as band C and on values of P_o determined from excised, inside-out patches of membrane. Nevertheless, the predicted and observed values agree well. Thus, these data provide a molecular explanation for the quantitative decrease in cAMP-stimulated apical membrane Cl^- current generated by A455E and P574H.

Table I. Comparison of predicted apical membrane Cl^- current, $N \times i \times P_o$, and measured cAMP-stimulated apical membrane Cl^- current, I^{Cl}(apical), for wild-type and mutant CFTR

	N (%)	i (%)	P_o (%)	$N \times i \times P_o$ (%)	I^{Cl}(apical) (%)
Wild-type	100	100	100	100	100
ΔF508	4	100	38	1.6	0
A455E	11	100	93	10.5	8
P574H	15	100	139	21.1	17

N, the number of Cl^- channels in the apical membrane; i, single-channel current; P_o, open-state probability. To estimate N relative to wild-type CFTR, we used the data shown in Figure 6B and let the value of wild-type CFTR equal 100%. For all other values, wild-type CFTR was assigned a value of 100%. P_o for ΔF508 is from Denning *et al.* (1992a); Dalemans *et al.* (1991) had a similar value.

Mechanism of altered gating by A455E and P574H

A455 and P574 lie near the conserved Walker A and B motifs of NBD1. These residues are conserved in CFTR from all species that have been sequenced and in several members of the traffic ATPase/ATP binding cassette (ABC) transporter family (Ames *et al.*, 1990; Hyde *et al.*, 1990). In ATP binding and hydrolyzing proteins, both motifs are important for binding ATP, and the highly conserved Walker A lysine and Walker B aspartate residues are essential for normal ATP hydrolysis.

P574H decreased β_1, a rate constant that is also controlled by ATP and which describes the transition to the bursting state. Because of the proximity of P574 to D572 (the Walker B aspartate of NBD1), we speculate that P574H alters the interaction of NBD1 with MgATP, and/or the consequences thereof, and hence slows the rate of channel opening. P574H also altered α_1. It is interesting to compare the effect that different mutations in NBD1 had on α_1: P574H decreased α_1, A455E did not change α_1, and K464A (a mutant of the Walker A lysine of NBD1; Carson and Welsh, 1995) appeared to increase the rate of channel closing. We speculate that the interaction of ATP with NBD1 affects not only the opening but also the closing of the channel. Further work is required to

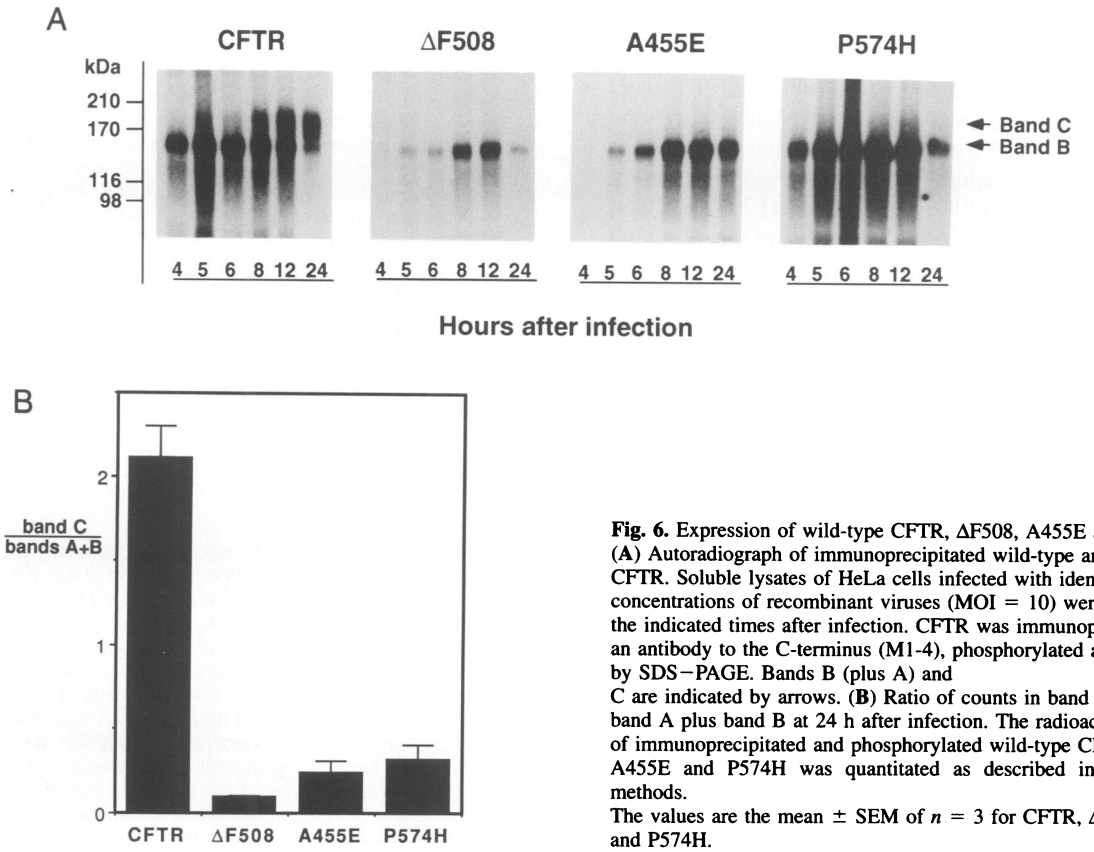

Fig. 6. Expression of wild-type CFTR, ΔF508, A455E and P574H. (**A**) Autoradiograph of immunoprecipitated wild-type and mutant CFTR. Soluble lysates of HeLa cells infected with identical concentrations of recombinant viruses (MOI = 10) were harvested at the indicated times after infection. CFTR was immunoprecipitated with an antibody to the C-terminus (M1-4), phosphorylated and separated by SDS−PAGE. Bands B (plus A) and C are indicated by arrows. (**B**) Ratio of counts in band C to counts in band A plus band B at 24 h after infection. The radioactivity in gels of immunoprecipitated and phosphorylated wild-type CFTR, ΔF508, A455E and P574H was quantitated as described in Materials and methods.
The values are the mean ± SEM of $n = 3$ for CFTR, ΔF508, A455E and P574H.

understand how CFTR is regulated by the NBDs and to learn how P574H alters this function.

It is interesting that A455E appeared to increase β_2 and α_2, thereby increasing the frequency of transitions within a burst of activity. Our previous work suggested that the transition from C_1 to the bursting state ($C_2 \Leftrightarrow O$) was controlled by an interaction with ATP (Winter *et al.*, 1994). Our data from A455E, plus the finding that P574H altered β_2, suggest that the NBDs may also be involved in regulating gating within a burst. One possible interpretation of the effect of A455E is that the mutation reduced the height of an energy barrier between the short-lived closed state (C_2) and the open state.

Cellular processing of A455E and P574H

An important mechanism of dysfunction of CFTR containing CF-associated mutations is misprocessing, so that the mutant protein fails to leave the endoplasmic reticulum and traffic to the Golgi complex and then on to the cell surface (Cheng *et al.*, 1990). Previous studies have demonstrated that a number of mutants, most notably ΔF508, are misprocessed. As a result, there is little appreciable protein at the cell surface (Cheng *et al.*, 1990; Gregory *et al.*, 1991; Denning *et al.*, 1992b; Kartner *et al.*, 1992). Prior to this study, all mutations known to manifest a processing defect have been associated with the severe PI clinical phenotype. Our data indicate that processing mutations are not necessarily an all-or-none defect; in contrast to ΔF508, some of the mutant A455E and P574H protein had a glycosylation pattern consistent with processing in the Golgi complex and generated cAMP-stimulated apical Cl^- currents.

We evaluated the processing of A455E and P574H in HeLa and FRT cells incubated at 37°C. Previous studies have shown that when cells stably expressing the ΔF508 mutant are incubated at reduced temperature (23–30°C), the processing of ΔF508 reverts partially towards that of wild-type (Denning *et al.*, 1992a). It is interesting to speculate that a reduction in temperature might increase the processing of these mutants even more than that of the ΔF508 mutant.

The present data indicate that the structural requirements for channel function are distinct from the requirements for protein processing. For example, A455E formed a channel that was misprocessed yet had conductive and regulatory properties very similar to those of wild-type CFTR. More strikingly, P574H, which was also misprocessed, formed a channel that was even more active than wild-type. Thus, normal or supernormal Cl^- transport by CFTR is not in itself sufficient for normal processing. Conversely, previous data have shown that some mutants, such as G551D, have little Cl^- channel function, yet are processed correctly (Cheng *et al.*, 1990; Kartner *et al.*, 1992). Thus, the Cl^- channel function of CFTR is neither required nor sufficient for normal processing through the Golgi complex. It is interesting that mutations which must confer upon CFTR a structure that is recognized as abnormal by the cellular quality control system have such minor effects on the function of the channel.

Implications for cystic fibrosis

These data suggest that the mutations A455E and P574H cause CF because they disrupt the processing of CFTR and its delivery to the cell surface. However, they also suggest that these mutations are associated with a milder (PS) clinical phenotype because a small amount of the

mutant protein is processed correctly, retains normal or greater than normal Cl^- channel function and thus generates residual cAMP-stimulated apical membrane Cl^- currents. These conclusions are consistent with the observations of Veeze *et al.* (1994) who demonstrated that rectal biopsies from patients bearing the A455E mutation retain residual Cl^- secretion. Veeze *et al.* (1994) and Gan *et al.* (1994) found that patients with the A455E mutation were PS, but it is not clear whether or not the A455E mutation confers milder lung disease. Uncertainty about the severity of lung disease in these patients highlights the difficulty in assessing the clinical phenotype associated with the A455E and P574H mutations in relatively small numbers of patients. Thus, caution is warranted when relating genotype, biochemical abnormality and clinical phenotype.

It is interesting to compare our present results with those from our study of mild CF mutations that occur in MSD1 (R117H, R334W and R347P). We showed that when expressed in FRT epithelia, those mild mutants generated 15, 4 and 33%, respectively, of the current generated by wild-type CFTR (Sheppard *et al.*, 1993). These values are in the same range as those found for A455E (8%) and P574H (17%). Thus, it would appear that no matter what the specific mechanism of dysfunction, a small amount of residual CFTR function at the membrane is sufficient to confer a milder clinical phenotype. A correlate of this conclusion would be that the major abnormalities and the clinical phenotype in CF are not due to the presence of misprocessed protein or the abnormal location of functional protein.

A455E or P574H could prove to be of value in the development of therapies designed to augment the delivery to and the retention of mutant protein at the plasma membrane (Cheng *et al.*, 1990; Lukacs *et al.*, 1993). Although ΔF508 could be used to assess the processing defect, A455E or P574H might prove to be more tractable models for evaluating strategies to correct mislocalization because the processing defect is only partial and the conductance and regulation of the Cl^- channels is more nearly normal. We have suggested previously that pharmacological therapies designed to increase the activity of mutant protein present in the plasma membrane might be effective in patients bearing mutations in the MSDs (Sheppard *et al.*, 1993). Such strategies might also be applied to patients bearing the A455E and P574H mutations because they appear to have at least some functional protein present in the plasma membrane.

Materials and methods

Site-directed mutagenesis

CFTR mutants were constructed in the vaccinia virus expression plasmid pTM1-CFTR4 (Cheng *et al.*, 1990), as described previously (Kunkel, 1985; Gregory *et al.*, 1990). Mutants are named by their single-letter amino acid code and their position within the CFTR sequence, followed by the specific mutation. The DNA sequences of the mutants were examined to verify that the glycosylation sites were intact and that F508 was present.

Cells and CFTR expression systems

We transiently expressed wild-type and mutant CFTR in FRT and HeLa cells using the vaccinia virus–bacteriophage T7 hybrid expression system (Elroy-Stein *et al.*, 1989; Rich *et al.*, 1990). We used a double-infection protocol, with one recombinant virus expressing the bacteriophage T7 RNA polymerase and a second recombinant virus containing either wild-type or mutant CFTR cDNA under the control of the T7 promoter (Anderson *et al.*, 1991). In some experiments we used the cationic lipid Lipofectin (Life Technologies Inc., Gaithersburg, MD) to transfect vTF7-3-infected cells with either wild-type or mutant CFTR plasmid. Similar results were obtained with both methods; the data were combined. Cells were maintained in culture and recombinant vaccinia viruses expressing wild-type and mutant CFTR were prepared as described previously (Rich *et al.*, 1990; Anderson *et al.*, 1991; Sheppard *et al.*, 1994a).

Polarized FRT epithelia with high transepithelial resistances (day 5 after seeding) were infected with equivalent multiplicity of infections (MOI = 5) of vTF7-3 and either wild-type or mutant CFTR, as described previously (Sheppard *et al.*, 1993, 1994a). HeLa cells (60–80% confluent, 8–24 h after seeding) were infected with an MOI of 10–20. Medium containing recombinant vaccinia viruses or Lipofectin and plasmid was removed after 4–6 h and replaced with fresh medium. For protein expression studies, cell lysates were harvested at the indicated times after infection; for electrophysiology, cells were assayed for Cl^- channel function 8–32 h after infection.

Electrophysiology

Apical membrane Cl^- current [I^{Cl}(apical)] was measured as described previously (Anderson and Welsh, 1991; Sheppard *et al.*, 1993, 1994a). The apical membrane of FRT epithelia was bathed in a solution containing (in mM): 135 NaCl, 1.2 $CaCl_2$, 1.2 $MgCl_2$, 2.4 K_2HPO_4, 0.6 KH_2PO_4, 10 HEPES and 10 dextrose (titrated to pH 7.4 with NaOH). The composition of the basolateral solution was similar to the apical solution, with the exception that 135 mM Na gluconate replaced 135 mM NaCl, to give a Cl^- concentration of 4.8 mM. Solutions were maintained at 37°C and bubbled with O_2. Nystatin (0.36 mg/ml) was added to the basolateral solution to permeabilize the basolateral membrane. Transepithelial voltage (referenced to the apical solution) was clamped at 0 mV, and apical Cl^- current was recorded continuously. Under these conditions, cAMP-stimulated current results from Cl^- flow-through apical membrane CFTR Cl^- channels (Anderson and Welsh, 1991; Sheppard *et al.*, 1993, 1994a). Flow of Cl^- from the apical to the basolateral solution is shown as an upward current deflection.

Whole-cell and single-channel currents were recorded, as described previously (Hamill *et al.*, 1981; Sheppard *et al.*, 1993). Experiments were conducted at 34–36°C. The established sign convention was used throughout. Liquid junction potentials and potentials at the tip of the patch pipette were measured and $I-V$ relationships corrected for the corresponding offset.

For whole-cell experiments the pipette (internal) solution contained (in mM): 120 *N*-methyl-D-glucamine (NMDG), 85 aspartic acid, 3 $MgCl_2$, 1 ethyleneglycol-bis-(β-aminoethylether) *N,N,N',N'*,-tetraacetic acid cesium salt (CsEGTA), 1 MgATP and 5 *N*-Tris(hydroxymethyl) methyl-2-aminoethane sulfonic acid (TES), pH 7.3, with HCl ($[Cl^-]$ = 43 mM; $[Ca^{2+}]_{free} < 10^{-8}$ M). The bath (external) solution contained (in mM): 140 NaCl, 1.2 $MgSO_4$, 1.2 $CaCl_2$, 10 dextrose and 10 TES, pH 7.3, with NaOH ($[Cl^-]$ = 142 mM). Whole-cell currents, filtered at 0.5 kHz and digitized at 2 kHz, have not been capacitance- or leakage-subtracted.

For experiments with excised inside-out membrane patches, the pipette (extracellular) solution contained (in mM): 140 NMDG, 140 aspartic acid, 5 $CaCl_2$, 2 $MgSO_4$ and 10 TES, pH 7.3, with Tris ($[Cl^-]$ = 10 mM). The bath (intracellular) solution contained (in mM): 140 NMDG, 3 $MgCl_2$, 1 CsEGTA and 10 TES, pH 7.3, with HCl ($[Cl^-]$ = 147 mM; $[Ca^{2+}]_{free} < 10^{-8}$ M). Single-channel currents were filtered at 0.5–1.0 kHz and digitized at 5–10 kHz. Single-channel current amplitudes were determined from the fit of Gaussian distributions to current amplitude histograms. The fit of linear least squares regression lines to single-channel $I-V$ relationships was used to determine single-channel conductance at negative voltages, where the $I-V$ relationship was linear (Sheppard *et al.*, 1993). Single-channel P_o was measured in patches containing four or less channels and in current recordings of at least 100 s duration. The number of channels in each patch was determined from the maximum number simultaneously open with 2.27 mM MgATP in the intracellular solution after PKA-dependent phosphorylation. Data were analyzed using pClamp software (Axon Instruments Inc., Foster City, CA).

Maximum likelihood analysis and kinetic modeling

Maximum likelihood analysis and kinetic modeling were performed using data from membrane patches that contained only a single active channel, as described previously (Winter *et al.*, 1994). Briefly, unfiltered

single-channel data were digitized on a microcomputer (Apple Macintosh, Apple Computer Inc., Cupertine, CA) equipped with a multifunctional data acquisition board (NB-MIO-16) and LabVIEW 3 software (National Instruments, Austin, TX) at 5 kHz following filtering with an 8-pole Bessel filter (Frequency Devices Inc., Haverhill, MA) at a corner frequency of 1 kHz with subsequent digital filtering at 500 Hz. Our previous studies have shown that a linear three-state model ($C_1 \Leftrightarrow C_2 \Leftrightarrow O$) best describes the kinetic behavior of CFTR Cl^- channels (Winter *et al.*, 1994). The Maple 5 symbolic algebra program (Waterloo Maple Software, Waterloo, Canada) was used to derive the open and closed time probability density functions for this model by solving the matrix equations in terms of the rate constants. The resulting equations were used in LabVIEW 3 to determine the set of rate constants which yielded the maximum likelihood for the open and closed times observed.

Processing

For the time course of production of band C, we infected FRT and HeLa cells which had reached 80–90% confluency with the recombinant vaccinia viruses, vTF7-3 and the indicated CFTR mutant at 10 MOI each, as described above. Cells were harvested at the indicated times after infection, washed three times with ice-cold PBS (150 mM NaP_i)/phenylmethylsulfonyl fluoride (0.1 mM PMSF) and solubilized in 1% digitonin in lysis buffer (50 mM Tris, pH 7.4, 150 mM NaCl, 2 μg/ml aprotinin and 0.1 mM PMSF). Soluble proteins were collected as the supernatant from a 200 000 *g* spin and stored at −70°C until all time points were harvested.

Wild-type and mutant CFTR were immunoprecipitated from the soluble fraction with the monoclonal antibody M1-4 (which recognizes the C-terminus of CFTR; Denning *et al.*, 1992b), and *in vitro*-phosphorylated with the catalytic subunit of PKA and [γ-^{32}P]ATP (Cheng *et al.*, 1990; Gregory *et al.*, 1990). Washed precipitates were electrophoresed on 6% SDS−PAGE, dried and autoradiographed. Dried gels were quantitated by radioanalytic scanning (AMBIS Systems Inc., San Diego, CA).

Reagents

The recombinant vaccinia virus (vTF7-3), which expresses the bacteriophage T7 RNA polymerase, was purchased from American Type Culture Collection (Rockville, MD). PKA was obtained from Promega (Madison, WI) and [γ-^{32}P]ATP was purchased from New England Nuclear Research Products (Boston, MA). MgATP, Na_2ATP, CPT-cAMP sodium salt, forskolin and 3-isobutyl-1-methylxanthine (IBMX) were obtained from Sigma Chemical Company (St Louis, MO). All other chemicals were of reagent grade.

Statistics

Results are expressed as the mean ± SEM of *n* observations. To compare mean values, we used Student's *t*-test. Differences were considered statistically significant when the *P* value was <0.05.

Acknowledgements

We thank S.P.Weber, L.G.DeBerg, P.H.Karp, D.R.Ries, S.R.Struble, J.A.Cieslak and E.C.Kasik for excellent technical assistance and T.A.Mayhew and D.R.Vavroch for secretarial help. We thank our laboratory colleagues and collaborators for their advice and critical comments. We also thank the DNA Core, University of Iowa, for oligonucleotide synthesis and DNA sequencing, and the Hybridoma Facility, University of Iowa, for antibody production. FRT cells were a generous gift from Dr C.Zurzolo, Cornell University Medical College, New York. This work was supported by the Howard Hughes Medical Institute, the National Heart Lung and Blood Institute and the Cystic Fibrosis Foundation.

References

Ames,G.F.-L., Mimura,C.S. and Shyamala,V. (1990) *FEMS Microbiol. Rev.*, **75**, 429–446.

Anderson,M.P. and Welsh,M.J. (1991) *Proc. Natl Acad. Sci. USA*, **88**, 6003–6007.

Anderson,M.P. and Welsh,M.J. (1992) *Science*, **257**, 1701–1704.

Anderson,M.P., Berger,H.A., Rich,D.P., Gregory,R.J., Smith,A.E. and Welsh,M.J. (1991) *Cell*, **67**, 775–784.

Carson,M. and Welsh,M.J. (1995) *J. Biol. Chem.*, **270**, 1711–1717.

Cheng,S.H., Gregory,R.J., Marshall,J., Paul,S., Souza,D.W., White,G.A., O'Riordan,C.R. and Smith,A.E. (1990) *Cell*, **63**, 827–834.

Collins,F.S. (1992) *Science*, **256**, 774–779.

Dalemans,W. *et al.* (1991) *Nature*, **354**, 526–528.

Denning,G.M., Anderson,M.P., Amara,J., Marshall,J., Smith,A.E. and Welsh,M.J. (1992a) *Nature*, **358**, 761–764.

Denning,G.M., Ostedgaard,L.S. and Welsh,M.J. (1992b) *J. Cell Biol.*, **118**, 551–559.

Elroy-Stein,O., Fuerst,T.R. and Moss,B. (1989) *Proc. Natl Acad. Sci. USA*, **86**, 6126–6130.

Gan,K.H., Heijerman,H.G.M. and Bakker,W. (1994) *N. Engl. J. Med.*, **330**, 865–866.

Gregory,R.J. *et al.* (1990) *Nature*, **347**, 382–386.

Gregory,R.J., Rich,D.P., Cheng,S.H., Souza,D.W., Paul,S., Manavalan,P., Anderson,M.P., Welsh,M.J. and Smith,A.E. (1991) *Mol. Cell. Biol.*, **11**, 3886–3893.

Hamill,O.P., Marty,A., Neher,E., Sakmann,B. and Sigworth,F.J. (1981) *Pflugers Arch.*, **391**, 85–100.

Hyde,S.C. *et al.* (1990) *Nature*, **346**, 362–365.

Kartner,N., Augustinas,O., Jensen,T.J., Naismith,A.L. and Riordan,J.R. (1992) *Nature Genet.*, **1**, 321–327.

Kerem,B.S. *et al.* (1990) *Proc. Natl Acad. Sci. USA*, **87**, 8447–8451.

Kristidis,P., Bozon,D., Corey,M., Markiewicz,D., Rommens,J., Tsui,L.-C. and Durie,P. (1992) *Am. J. Hum. Genet.*, **50**, 1178–1184.

Kunkel,T.A. (1985) *Proc. Natl Acad. Sci. USA*, **82**, 488–492.

Lukacs,G.L., Chang,X.-B., Bear,C., Kartner,N., Mohamed,A., Riordan,J.R. and Grinstein,S. (1993) *J. Biol. Chem.*, **268**, 21592–21598.

Nitsch,L. and Wollman,S.H. (1980) *Proc. Natl Acad. Sci. USA*, **77**, 472–476.

Rich,D.P. *et al.* (1990) *Nature*, **347**, 358–363.

Riordan,J.R. (1993) *Annu. Rev. Physiol.*, **55**, 609–630.

Riordan,J.R. *et al.* (1989) *Science*, **245**, 1066–1073.

Rozen,R. *et al.* (1992) *Am. J. Med. Genet.*, **42**, 360–364.

Sheppard,D.N., Rich,D.P., Ostedgaard,L.S., Gregory,R.J., Smith,A.E. and Welsh,M.J. (1993) *Nature*, **362**, 160–164.

Sheppard,D.N., Carson,M.R., Ostedgaard,L.S., Denning,G.M. and Welsh,M.J. (1994a) *Am. J. Physiol.*, **266**, L405−L413.

Sheppard,D.N., Ostedgaard,L.S., Rich,D.P. and Welsh,M.J. (1994b) *Cell*, **76**, 1091–1098.

Smit,L.S., Wilkinson,D.J., Mansoura,M.K., Collins,F.S. and Dawson,D.C. (1993) *Proc. Natl Acad. Sci. USA*, **90**, 9963–9967.

Tabcharani,J.A., Rommens,J.M., Hou,Y.X., Chang,X.-B., Tsui,L.-C., Riordan,J.R. and Hanrahan,J.W. (1993) *Nature*, **366**, 79–82.

The Cystic Fibrosis Genotype−Phenotype Consortium (1993) *N. Engl. J. Med.*, **329**, 1308–1313.

Veeze,H.J., Halley,D.J.J., Bijman,J., de Jongste,J.C., de Jonge,H.R. and Sinaasappel,M. (1994) *J. Clin. Invest.*, **93**, 461–466.

Walker,J.E., Saraste,M., Runswick,M.J. and Gay,N.J. (1982) *EMBO J.*, **1**, 945–951.

Welsh,M.J. *et al.* (1992) *Neuron*, **8**, 821–829.

Welsh,M.J., Boat,T.F., Tsui,L.-C. and Beaudet,A.L. (1995) In Scriver,C.R., Beaudet,A.L., Sly,W.S. and Valle,D. (eds), *The Metabolic Basis of Inherited Disease*. McGraw-Hill Press Inc., New York, Vol. III, pp. 3799–3876.

Winter,M.C., Sheppard,D.N., Carson,M.R. and Welsh,M.J. (1994) *Biophys. J.*, **66**, 1398–1403.

Received on October 17, 1994; revised on December 9, 1994